Fabrication of metallic magnetic nanostructures by argon ion milling using a reversed polarity planar magnetron ion source

A.T. Hindmarch[a,b,*], D.E. Parkes[a], A.W. Rushforth[a]

[a]School of Physics & Astronomy, University of Nottingham, Nottingham, NG7 2RD UK
[b]Centre for Materials Physics, Durham University, South Road, Durham, DH1 3LE UK

Abstract

We demonstrate that a planar magnetron may be used as a source of ions for milling micro- and nanostructured devices. Reversing the polarity of the magnetron head, in combination with applying a voltage bias to the thin-film sample, allows acceleration of ions produced in the Ar glow-discharge to energies suitable for pattern transfer via etching. We have fabricated generic Hall-bar and nanowire L-bar structures from sputter deposited Ta/Ni/Ta trilayer films grown onto clean GaAs(001) surfaces. No degradation of the magnetic properties or contamination of the deposition chamber vacuum are observed, demonstrating that this method is effective for etching magnetic device structures patterned by both optical and electron-beam lithography techniques.

Keywords: Argon ion milling; microfabrication; lithography
PACS: 52.77.Bn, 81.16.Rf, 85.40.Hp

Ar ion milling is a pattern-transfer technique which, in conjunction with optical and electron-beam lithography processing, is now commonplace in micro- and nano-fabrication [1–3]. For metallic or metal-oxide nanostructures, e.g., metallic nanowires [4, 5] and arrays [6], magnetic tunnel junctions [7, 8] or Josephson junction [9] structures, and in other situations where lift-off techniques are inappropriate, Ar ion milling is often preferable to the wet chemical- or reactive ion etching often used for semiconductor devices. Reactive chemical etching techniques such as these are usually unsuitable for patterning devices comprising metals and/or insulating oxides/nitrides due to problems in obtaining sufficiently high-quality edge definition, controllable ramp-junction profiles, and avoiding detrimental sidewall reactions. The ion milling fabrication step is performed using a dedicated system employing a broad-beam RF or DC ion source to generate a beam of (usually) Ar ions with beam energy typically in the range 600-1000 eV. This ion beam is used to etch away any regions of the thin-film or device heterostructure which are left unprotected by an overlying resist pattern. However, stand-alone ion milling systems are not always available, particularly in cleanroom processing suites primarily used for semiconductor device microfabrication.

A review of gridded and gridless broad-beam ion-source technologies, for both surface modification and space-propulsion, is given by Kaufman [10], and gridless ion sources based on gas jet injection through a planar magnetron array are available commercially from several companies including General Plasma [11] and Gencoa [12]. Recently, Ranjan *et al.* have demonstrated that applying a reversed bias to a planar magnetron sputter source — turning the discharge cathode into an
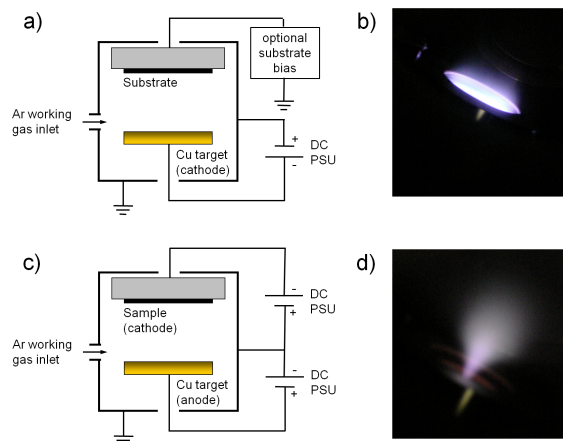
Figure 1: Color online: Schematic diagrams of the biasing applied to the magnetron head and sample table during a) sputter deposition and c) Ar ion milling. Photographs of the resulting glow-discharges are shown in b) and d), respectively.

anode — allows such a source to be used to produce Ar ions [13]. In this article we demonstrate that an Ar ion beam created by the discharge from a reversed polarity planar magnetron source in a conventional magnetron sputter deposition system may be used for fabricating thin-film magnetic micro- and nanostructures by Ar ion milling.

A Mantis QPrep500 ultra-high vacuum (UHV) sputter deposition system with base-pressure better than 6.67×10^{-7} Pa (5×10^{-9} Torr) was used to deposit the thin-film structures from which the devices were fabricated, and subsequently to Ar ion mill the patterned devices. The thin-film structure was grown by DC magnetron sputtering in an Ar working gas pressure of 0.13 Pa (1 mTorr) at growth-rates of ∼0.03 nm/s and a target-

*Corresponding author
Email address: a.t.hindmarch@durham.ac.uk (A.T. Hindmarch)

substrate distance of 200 mm. The substrate was electrically grounded during sputter deposition. The sample table was rotated at 20 rpm during both deposition and milling, in order to ensure uniformity over the wafer area and avoid shadowing. For Ar ion milling, as suggested in reference [13], to provide a source of Ar ions we reversed the polarity of the bias voltage applied to one of the magnetron heads, as shown schematically in figure 1c). The magnetron head had a balanced-mode toroidal-field magnet geometry, and a 50 mm diameter Cu sputter target was arbitrarily chosen as the discharge anode. A 250 V positive bias applied to the magnetron head in a 0.2 Pa (1.5 mTorr) Ar atmosphere generated an 8W plasma discharge [figure 1d)] with the substrate shutter closed and in the absence of a bias applied to the sample manipulator. Due to the polarity of the bias applied, no Ar ions were accelerated toward the sputter target (anode); and hence no sputter deposition from the target occurred. Opening the sample shutter and applying a further *negative* bias of 630 V to the substrate manipulator caused an increase in the discharge power to ~ 20 W, and Ar ions to be accelerated toward the substrate manipulator; at which point milling of the patterned devices commenced.

In reference [13], Ranjan *et al.* found that the ion energy spread was reduced at higher discharge voltage and lower Ar pressure: herein lies a compromise which we must make when using this method of Ar ion generation. During ion milling of structures defined by a resist pattern, it is critical that the sample temperature is not significantly raised during milling — raising the temperature can have the detrimental effect of indelibly 'baking' the resist to the sample surface; making it problematic to remove afterwards, and preventing reliable electrical contacts from being made to the patterned device. In the typical Kaufman-type [14] DC, or RF, ion source, the ion energy is determined by the voltages applied to the extraction- and accelerator-grid arrays downstream of the discharge plasma, providing a controlled monoenergetic ion beam. The parameters used here in generating the plasma discharge, 250 V applied bias in 0.2 Pa Ar, whilst likely resulting in a broadening of the ion energy distribution, produce an easily struck, highly stable, discharge and should prevent the plasma extending sufficiently far toward the sample manipulator to cause excessive heating. As described previously, acceleration of Ar ions toward the sample is achieved by applying negative bias to the substrate manipulator: this acts in a similar manner to the extraction- and accelerator-grids in a conventional ion source in that it (primarily) determines the energy with which Ar ions impinge upon the sample.

We discuss two types of generic magnetic nanostructured devices which we have fabricated: Hall-bar structures were patterned by conventional optical photolithography with BPRS-150 photoresist, and nanowire L-bar structures were patterned using PMMA 495K-A5 resist and a JEOL electron-beam lithography system which was also used to obtain scanning electron microscope (SEM) images of the completed L-bar structures. The devices consisted of a Ta[3 nm]/Ni[20 nm]/Ta[3 nm] trilayer stack deposited onto a segment of semi-insulating GaAs(001) wafer. Prior to thin-film deposition the GaAs substrate was chemically etched to remove the native surface oxide, then an-
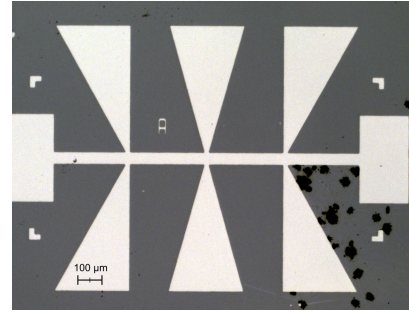
Figure 2: Optical micrograph showing a patterned Ta/Ni/Ta/GaAs Hall-bar structure. Dark features seen to the lower right of the image are a result of the acid etch/anneal procedure prior to film growth. A 100 μm scale-bar is shown to the lower left of the image.

nealed at 550 °C for 1 hr in the UHV system. The Ta/Ni/Ta trilayer was deposited once the substrate had cooled to 35 °C under UHV. The use of such high-temperature thermal treatment, in this case to produce a clean GaAs(001) surface prior to thin-film deposition, is clearly incompatible with simple lift-off-based micro- and nanofabrication techniques. The trilayer film sample was diced into smaller pieces which were then individually lithographically patterned. After patterning the resist layers, the samples were mounted onto a Cu backing plate with conducting silver-loaded paste and reintroduced to the sputter chamber for Ar ion milling. Residual gas analysis scans were taken before and after etching, using a SRS RGA-100 quadrupole residual gas analyzer (RGA) fitted with a Faraday-cup detector and having a scan-range up to 100 amu. In order to ascertain that no degradation of the magnetic properties of the films has occurred as a result of the milling method, longitudinal magneto-optic Kerr effect (MOKE) hysteresis measurements were made at ambient temperature using a focussed-MOKE magnetometer with a beam spot-diameter of ~ 3 μm at the sample, and with an alternating magnetic field applied at 21 Hz in the sample plane.

For larger-scale structures, such as optically patterned Hall-bars, one may determine the required milling time from visual inspection of the sample through the loadlock or chamber viewport – in order to determine when surrounding material is entirely milled away. For these structures a total milling time of 40 mins at a bias of 630 V was required, corresponding to an etch-rate of ~ 0.01 nm/s. Figure 2 shows an optical micrograph of a Hall-bar structure, defined using UV-photolithography and etched as described above. The device structure is well defined, both the Hall-bar structure itself and the corresponding alignment markers, indicating successful pattern transfer from the photomask and resist pattern to the film by milling using a reversed-polarity magnetron ion source. No resist residue remains on the surface of the patterned device, indicating that this method does not induce undue heating of the sample during milling. Damage to the substrate may be seen to the lower right of figure 2: This damage is, however, *below* the deposited Ta/Ni/Ta trilayer film, and thus must occur prior to film deposition and milling, during either the acid-etch or anneal stages of fabrication – this damage to the GaAs substrate is not caused
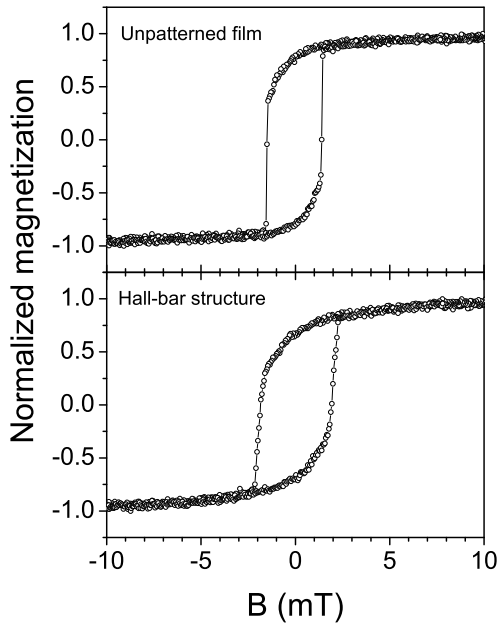
Figure 3: Room temperature focussed-MOKE hysteresis loops for Ta/Ni/Ta/GaAs sheet material (upper) and the cross-center in a Hall-bar structure (lower). After pattering the Ni film device remains ferromagnetic and the coercive field increases slightly.
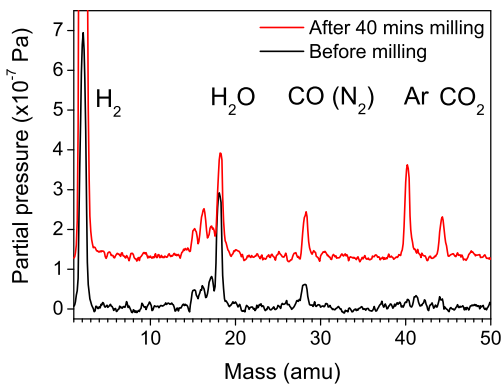
Figure 4: Color online: RGA scans showing the partial pressures of residual gasses in the vacuum chamber before (lower trace, darker) and after (upper trace, lighter) Ar-ion milling (40 mins at 630 V sample bias) of Ta/Ni/Ta/GaAs Hall-bar structures defined with BPRS-150 photoresist. Traces are offset for clarity and significant residual gas peaks are labelled.
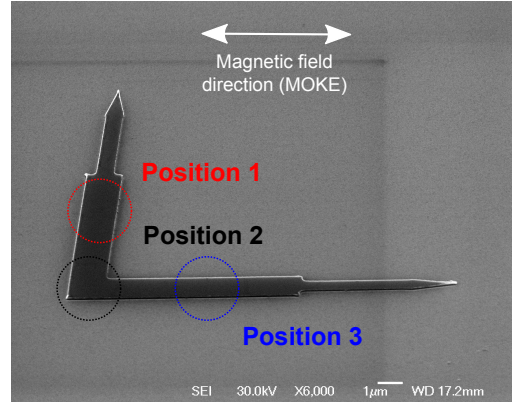
Figure 5: Color online:Scanning electron micrograph showing a patterned Ta/Ni/Ta/GaAs L-bar structure, viewed from a 45 ° angle from the substrate-normal. A 1 μm scale-bar is shown to the lower right of the image. The approximate size of the focussed-MOKE laser spot and positions where measurements were taken are indicated, as is the direction of the applied magnetic field during MOKE measurements.

by ion milling.

Figure 3 shows MOKE hysteresis loops for a region of unpatterned sheet material and a region in the middle of the central Hall-cross in a Hall-bar structure. The magnetic field during measurement is applied along the length of the Hall-bar. After patterning, the coercive field increases slightly, from 1.4 mT in the unpatterned film to 1.9 mT in the patterned Hall-bar, and the switching becomes less abrupt. These effects are caused by domain-wall pinning [15]: The interaction between magnetic domain-walls and the edges of the patterned structure slightly hinders domain-wall propagation, as is commonly observed in micro- and nanofabricated device structures [16]. The magnetic behavior of the patterned Hall-bar structure suggests that Ar ion milling optically patterned structures using the reversed-polarity magnetron technique does not have any significant detrimental effect on magnetic properties of the device.

A major concern when performing pattern transfer in a vacuum chamber designed for film growth is contamination of the growth chamber vacuum by resist residue; this has the potential to detrimentally impact on subsequent film growth. In order to confirm that no contamination of the chamber vacuum occurs after ion-milling, figure 4 shows RGA scans before and after Ar ion etching of Hall-bar structures defined by BPRS photoresist. Before milling there are peaks due to residual H_2, H_2O, CO and CO_2: Approximately 5 minutes after milling we find small increases in all of these residual gasses, plus residual Ar (inert process gas) – these residual gasses return to their initial levels within 1 hour. No further residual gas peaks are found at masses above 50 amu, e.g. complex hydrocarbon resist residues.

In order to verify that our Ar ion milling method allows transfer of patterns with smaller feature sizes we also fabricated L-bar structures patterned by electron-beam lithography. Figure 5 shows an SEM micrograph of such a structure, viewed from 45 ° from the sample normal. A lower bias voltage was used in this case in order to avoid excessive heating of the PMMA resist, which we have found occurs at higher bias. Etching for 40 mins, in this case at a sample-bias of 300 V rather

3
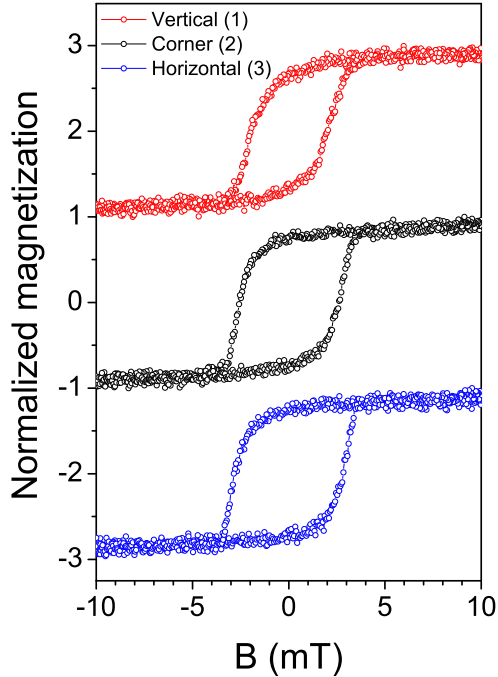
Figure 6: Color online: Room temperature focussed-MOKE hysteresis loops of a Ta/Ni/Ta/GaAs L-bar structure at different points, as indicated in figure 5. After patterning the Ni film device again remains ferromagnetic: The coercive field has increased further due to the decreased device dimensions, and a weak shape-anisotropy is apparent. Curves are vertically offset for clarity.

Figure 7: Color online: RGA scans showing the partial pressures of residual gasses in the vacuum chamber before (lower trace, darker) and after (upper trace, lighter) Ar ion milling (40 mins at 300 V sample bias) of Ta/Ni/Ta/GaAs L-bar structures defined with PMMA 495K-A5 e-beam resist. Traces are offset for clarity and significant residual gas peaks are, again, labelled.

than 630 V, again results in complete removal of excess material; suggesting that the milling rate is not strongly dependent on the applied bias voltage in the energy range utilized. One possible reason for this is that the ion energy may be limited due to collisions with neutral Ar process gas. We note that this method requires an Ar working-gas pressure of 0.2 Pa, whereas gridded ion sources typically operate at equivalent chamber pressures around 0.03 Pa or less; in a standard ion milling procedure, ions travel ballistically from source to sample, whereas in the case described here they will experience several collisions. The target–substrate distance is of order 5 mean-free-path lengths at our process pressure [17]. This may also explain the order of magnitude lower etch-rate here, in comparison to standard broad-beam ion milling.

The maximum width of the bar is 1 μm, dropping to 0.5 μm and then tapering to a point at each end. All features in the pattern have been transferred. No surface damage to the GaAs substrate is apparent from our SEM imaging, confirming that the features in figure 2 are not a result of the milling procedure. We comment also that, at this point, the use of an *in-situ* etch process makes it easy to back-fill around the patterned structures with insulating material, e.g. sputtered SiO_2, removing the need in some cases for an additional lithography step to open contacts in the dielectric barrier. However, for the structures described here we forego this step in order to avoid problems with sample charging during SEM imaging. It is trivial to introduce an Ar/O_2 mix in cases where etching with such a process gas may be appropriate.

Focussed-MOKE hysteresis loops were recorded on both
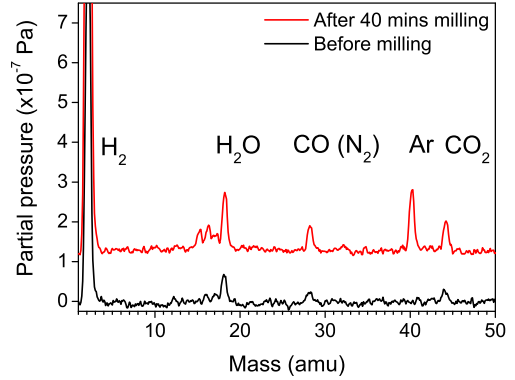
arms of the L-bar structure, the long axes of which are perpendicular and parallel to the applied field direction, and at the apex where the two arms join, as indicated in figure 5: These hysteresis loops are shown in figure 6. A further increase in coercive field is observed, due to the reduced device dimensions [16], and a weak shape anisotropy is observed — as may be expected, the magnetization preferentially lies along the axis of each arm of the L-bar structure.

Figure 7 shows RGA scans before and after Ar ion milling this L-bar structure at a sample bias of 300 V: Again, slight increases in residual H_2, CO, and CO_2 are observed shortly after milling, which again return to their initial levels after around 1 hour. Once again, we observe no heavier residual gas contamination of the growth-chamber vacuum. No additional contamination was observed when etching PMMA resist at 630 V bias, despite the resist baking to the film.

In summary, we have successfully etched both optical and electron-beam resist patterned device structures using a reverse-biased planar magnetron sputter source as a source of Ar ions. MOKE measurements confirm that the fabricated structures exhibit the anticipated magnetic properties, demonstrating that the films show no detrimental effects due to milling, and RGA scans show no contamination of the chamber vacuum from etching against either BPRS-150 or PMMA resist layers. This technique may be utilized as a viable, low-cost, alternative to dedicated broad-beam ion milling facilities for nanostructured device fabrication.

[1] A. Broers, Microelectron. Reliab. 4 (1) (1965) 103.

[2] C. M. Melliar-Smith, J. Vac. Sci. Technol. 13 (5) (1976) 1008.

[3] Y. Kitade, H. Komoriya, T. Maruyama, IEEE Trans. Mag. 40 (4) (2004) 2516.

[4] H. Tanigawa, T. Koyama, G. Yamada, D. Chiba, S. Kasai, S. Fukami, T. Suzuki, N. Ohshima, N. Ishiwata, Y. Nakatani, T. Ono, Appl. Phys. Express 2 (5) (2009) 053002.

[5] K. M. Seemann, Y. Mokrousov, A. Aziz, J. Miguel, F. Kronast, W. Kuch, M. G. Blamire, A. T. Hindmarch, B. J. Hickey, I. Souza, C. H. Marrows, Phys. Rev. Lett. 104 (7) (2010) 076402.

[6] Y. Kamata, A. Kikitsu, N. Kihara, S. Morita, K. Kimura, H. Izumi, IEEE Trans. Mag. 47 (1) (2011) 51.

[7] W. J. Gallagher, S. S. P. Parkin, Y. Lu, X. P. Bian, A. Marley, K. P. Roche, R. A. Altman, S. A. Rishton, C. Jahnes, T. M. Shaw, G. Xiao, J. Appl. Phys. 81 (8) (1997) 3741.

[8] H. X. Wei, Q. H. Qin, M. Ma, R. Sharif, X. F. Han, J. Appl. Phys. 101 (9) (2007) 09B501.

[9] D. H. A. Blank, H. Rogalla, J. Mater. Res. 12 (1997) 2952.

[10] H. R. Kaufman, Rev. Sci. Instrum. 61 (1) (1990) 230.

[11] http://www.generalplasma.com.

[12] http://www.gencoa.com.

[13] M. Ranjan, K. K. Kalathiparambil, N. P. Vaghela, S. Mukherjee, Plasma Process. Polym. 4 (2007) S1030.

[14] H. R. Kaufman, Advances in electronics and electron physics, Vol. 36, Academic, New York, 1974, p. 265.

[15] K. J. Dempsey, A. T. Hindmarch, D. A. Arena, C. H. Marrows, J. Magn. Magn. Mater. 322 (23) (2010) 3817.

[16] W. C. Uhlig, J. Shi, Appl. Phys. Lett. 84 (5) (2004) 759.

[17] D. J. Hucknall, A. Morris, Vacuum technology: calculations in chemistry, RSC, Cambridge, 2003.